

RECENT ADVANCES OF PHOTO-THERMAL SPECTROSCOPY

T. SAWADA and K. KATAYAMA

Graduate School of Frontier Sciences, The University of Tokyo
7-3-1 Hongo Bunkyo-ku, Tokyo 113-8656, Japan

ABSTRACT

Transient reflecting grating (TRG) measurements were applied to a silicon surface in the time range from femtoseconds to nanoseconds. Measurements with a time resolution of sub-nanoseconds provided a depth profiling of thermal and acoustic properties by changing the observed depth which is experimentally controllable. Two hundreds femtoseconds time-resolved measurements offer an investigation on initial processes of heat generation, that is, an energy transfer from electrons to phonons. Further, an ultrafast temperature change at a silicon surface was selectively and directly measured with a spectroscopic TRG method, so that the fundamental processes of heat generation can be investigated and also the signal can be used as a temperature indicator at a surface.

KEY WORDS

Transient grating, depth profiling, femtosecond, silicon

INTRODUCTION

In the latest device technology, device components get smaller and smaller to the size region of nanometers, and for example, thin films of several nanometers in thickness are practically used. As the size is reduced, the time of carrier transport between components also gets faster and faster to the time region of picoseconds. Ultrafast carrier transport generates heat in the nano-sized region, so that there are some local places with high temperature. To improve device performance, the fundamental physical processes of such heat generation at a surface or interface must be clarified and the temperature should be controlled. In order to clarify the origin of heat generation, the source processes, namely the photo-excited carrier dynamics should be studied. But comparatively there are not many such studies for silicon though it is one of the most fundamental device materials. For such studies, ultrafast photothermal methods can be used to observe carrier dynamics and the following heat generation. Transient reflecting grating (TRG) and Transient reflectivity (TR) are two of the ultrafast photothermal methods that have a detection region of several tens of nanometers.

We have developed TR and TRG methods for the last 10 years, and applied them to various solid surfaces^{1,2,3}, solid-liquid interfaces^{4,5,6,7}, multi-layered films⁸ and liquid surfaces⁹. In the time region of several nanoseconds, thermal and acoustic properties can be observed by the TRG technique. In this paper, we applied the TRG method to a silicon surface. First, sub-nanosecond time-resolved TRG method was applied to a silicon surface, and the physical meanings were considered. Next, the time resolution of the TRG method was improved to have a time resolution of 200 fs. Using this equipment, ultrafast carrier dynamics was measured for a silicon in order to get information on heat origin. Further, we adapted a femtosecond white-light continuum as a probe light in the TRG technique, so that the signal gives time-resolved spectroscopic information¹⁰. The spectroscopic TRG spectrum was analyzed to clarify the detailed carrier dynamics and the following heat generation.

EXPERIMENTAL

Schematic illustration of the principle for the TRG method is shown in Fig.1. In the TRG technique, two crossed pump pulses are incident at a solid surface and, as a result, the focused spot is irradiated with a pulse of an interference pattern. The complex refractive index at the spot changes due to a physical property change, or grating-patterned surface deformation occurs mainly due to a surface acoustic wave. After the pump pulses irradiation, a probe pulse is also incident there, and the complex refractive index change and the grating-patterned surface deformation are detected through the diffracted light of the probe light. A refractive index change due to photoexcited carriers is observed until several picoseconds, and that due to temperature rise is observed from several picoseconds to nanoseconds. A surface deformation is detected in the time range of several nanoseconds.

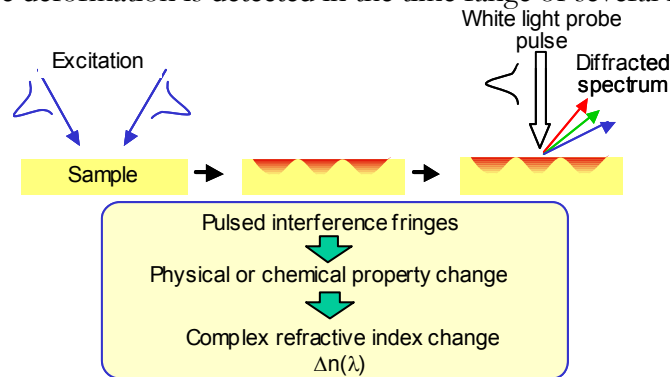


Fig.1 The principle of the transient reflecting grating method. The above figure corresponds in case of a white light pulses as probe pulses.

For measurement with a time resolution of sub-nanosecond, Nd-YAG laser (Pulse width :80 ps, Repetition frequency : 1 kHz, Wavelength : 1064 nm) was used as a light source. The wavelength was frequency-doubled to 532 nm. The pulse was separated into pump and probe pulses using a partial reflective mirror. The pump pulses were further divided into two pulses by a half mirror. The two pump pulses were crossed and irradiated onto the same spot of the sample surface, to coincide in time to form an interference pattern. The probe pulses were also incident at the spot after passing through a computer controlled optical delay line. The diffracted signal of the probe pulses were detected with a photomultiplier, and observed by a computer after averaging the signal with a box-car integrator.

In measurements with a time resolution of 200 fs, a regeneratively amplified titanium sapphire laser laser (CPA-1000; Clark-MXR Inc.) was used as a light source. The pulse train wavelength was 800 nm

with a repetition rate of 1 kHz and pulse width of 200 fs in full width at half maximum. Only the pump pulses were frequency doubled to a wavelength of 400 nm. The probe pulses remain 800 nm.

For spectroscopic measurements, the probe pulse was focused to a 10 mm thick cell filled with heavy water to generate a femtosecond white light continuum after passing through a computer controlled optical delay line. Used wavelengths ranged from 470 nm to 800 nm. The reflected diffracted light with a rainbow of colors spread like a fan due to the diffraction conditions. It was directed to the entrance of the optical fiber end after being collected and focused by lens. The diffraction spectrum was detected using the PMA-11 (HAMAMATSU) with a built-in spectroscope and CCD camera. The used sample was a single crystalline Si (111) without any dopants after etched in 1% HF aqueous solution for 5 minutes.

RESULTS AND DISCUSSION

TRG responses measured with the sub-nanosecond time resolution is shown in Fig.2. The signal had a small peak just after photo-excitation at the almost same time as incident pulse. The following signal shows an oscillating decay consisting of an exponential decay and an oscillating decay. The signal was separated to each component, which is shown in the right side of Fig.2.

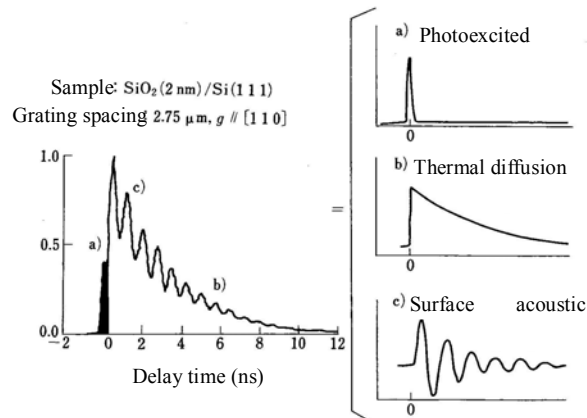


Fig.2 A response of transient reflecting grating for a silicon surface with a time resolution of 100ps. Three components comprising the response are also shown.

Considering the time range observed, the first peak corresponds to a refractive index change due to photo-excited carriers, and the exponential decay and the oscillating decay mean a thermal decay and a surface acoustic wave (SAW), respectively. It is very difficult to discuss the photo-excited carrier dynamic because the dynamics is considered to be faster processes than the used pulse width. About the thermal component, the decay occurs due to a thermal diffusion parallel to the interface, which disappears the temperature distribution like a grating pattern. Thus the decay time corresponds to the time during which heat diffuses for the length of the grating spacing. The grating spacing, Λ is expressed as $\Lambda = \lambda / 2 \sin(\theta/2)$, where λ is the wavelength of the pump pulses, and θ is the intersection angle of the two pump pulses. From the thermal decay time and the value of Λ , a thermal diffusion coefficient can be calculated, and this value is a property value in the depth region of Λ , which can be controlled by changing θ and has a typical length of 1 – 10 μm. Then, this signal provides a depth profiling of the thermal diffusion coefficient. The acoustic oscillation of the SAW originates in thermal expansion due to heat generation with a grating pattern. The wavelength of SAW must agree with the

grating spacing, so that the SAW with a controllable wavelength can be generated and detected. Since a SAW have an elastic information in a surface region of the wavelength, this acoustic signal also offers a depth profiling of elastic properties.

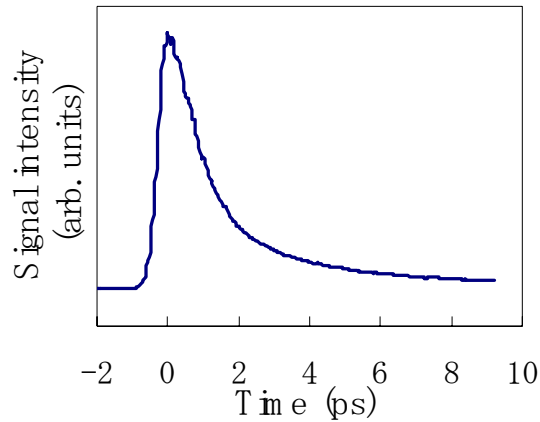


Fig.3 A response of transient reflecting grating for a silicon surface with a time resolution of 200fs. Three components comprising the response are also shown.

Next, the photoexcited carrier dynamic was focused on. The dynamics was observed in the first peak of the sub-nanosecond time-resolved TRG signal. To clarify the temporal response, the TRG measurement with the time resolution of 200 fs was applied to the same sample. The TRG response is shown in Fig.3. The signal rose just after photo-excitation and decayed in 2ps. The photo-excited carriers lose their energy due to scattering by phonons, that is, an energy transfer from photo-excited electrons to phonons. The process is the origin of a temperature rise. In the literature¹¹, it was reported that the scattering due to phonons occurs about a few picoseconds. Thus it was concluded that the TRG signal in the picoseconds time range includes information on the origin of heat generation, that is, an energy transfer from photo-excited electrons to phonons. But it makes difficult to analyze the signal that it has only a time-dependent response detected with a probe wavelength, though the signal consists of many time-dependent physical processes such as carrier-phonon (c-p) scattering, carrier diffusion, thermal diffusion, Auger recombination, trapping to surface states and so on.

In order to get more detailed information on the ultrafast dynamics, we adapted a femtosecond white-light continuum as a probe light in the TRG technique, so that the signal gives time-resolved spectroscopic information¹². This improvement provided detailed information on the excited state of photo-excited carriers and thermal properties.

TRG spectrums for a silicon until 20 ps and 300 ps are shown in Figs.4 (a) and (b), respectively. Looking at the Fig.1(a), the intensity of the TRG spectrum rose in the observed whole spectral range just after irradiation of the pump pulses, and decreased in a few picoseconds. After the decay, the spectrum intensity increased again only below the probe wavelength of 550 nm, and remains almost constant until 20 ps. From the Fig.1(b), the component decayed about 300 ps.

The faster decay in a few picoseconds is considered to correspond to a relaxation of photoexcited carriers due to carrier-phonon (c-p) scattering and carrier diffusion. Here, the slower component observed below 550 nm was investigated in detail. As mentioned in the experimental section, a permittivity change at a solid surface is measured by a TRG technique. Investigating what physical

processes induced the wavelength-dependent dielectric function change ($\Delta\epsilon(\lambda)$) in the time range of 300 ps. There is a possibility of carrier density change at a specific energy state in a bulk silicon. In case there is an interband transition in the probe wavelength range, a change in carrier density at the states related to the interband transition brings about a dielectric function change around the wavelength of the interband transition. But interband transitions for silicon lies at 3.4, 3.4 and 4.3 eV for L, Γ and X, respectively^{13,14}, that is, no interband transitions in the used probe wavelength range. Next possibility is carrier density change at a surface state. For silicon surfaces, various surface states are known and the energy positions were investigated mainly by the photoemission spectroscopy^{15,16,17}. Carrier dynamics at several types of surface states were investigated in the literature^{18,19,20}, and the results indicate that trapped carriers at surface states show a different behavior about a decay time and energy states only by changing the structure of the first layer. But no difference of the TRG spectrums was observed for a hydrogen-terminated and oxidized silicon surface. Thus this possibility is also denied. The left possibility is a temperature rise. It is reported that a temperature rise induces a wavelength dependent dielectric function change. Considering the signal intensity increased in a few picoseconds, the rise time agrees well with that for a temperature rise for general semiconductors. Further, the profile of the observed TRG spectrum was compared with that of a dielectric function change spectrum for various temperatures. The profile of the observed TRG spectrum resembled that of the permittivity change spectrum. Thus, it was concluded that the observed TRG spectrum is induced by a temperature rise at the silicon surface. This observation is the first one that provides a direct and selective measurement of ultrafast temperature change at a solid surface by selecting a transient response at an appropriate wavelength. Analyzing the TRG spectrums until a few picoseconds, the origin of heat generation can be studied, for example, carrier-carrier, c-p, defect scattering and so on. Further, the signal decay can be used as an in-situ indicator of temperature at a solid surface.

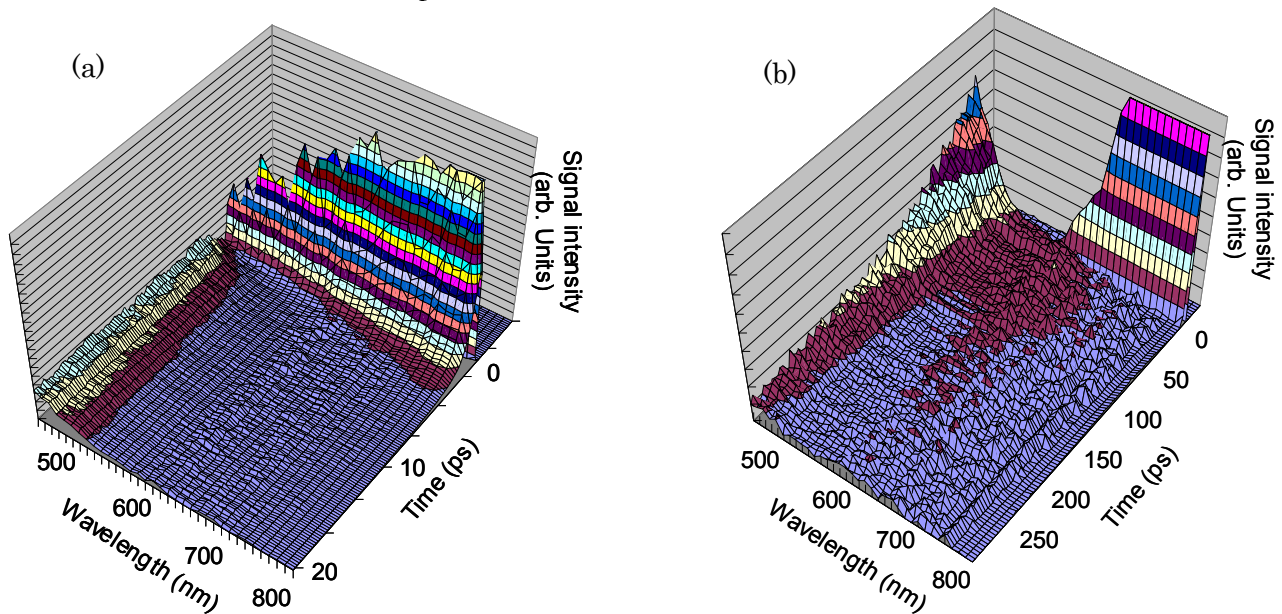


Fig.4 Three dimensional TRG spectrums for a silicon surface until 20 ps (a) and 300 ps (b). The probe wavelength ranges from 470 to 800 nm.

CONCLUSION

The TRG method was applied to a silicon surface in the time range from femtoseconds to nanoseconds. In a measurement with a time resolution of sub-nanoseconds, the signal gave

information on thermal diffusion and SAW. This method provides a depth profiling of thermal and acoustic properties by changing the experimentally controllable observed depth. Ultrafast time-measurement with 200fs time resolution offers an investigation of an initial heat generation, that is, an energy transfer from electrons to phonon. It was proved that the TRG spectrum below 550 nm shows a temperature rise and decay. This signal provides direct and selective temperature measurement at a solid surface, so that the fundamental processes of heat generation can be investigated and also the signal can be used as a temperature indicator at a surface.

REFERENCES

- ¹ K. Katayama, Q. Shen, A. Harata and T. Sawada, *Appl. Phys. Lett.* **69**, p. 2468 (1996).
- ² K. Katayama, Q. Shen, A. Harata and T. Sawada, *Phys. Rev. B* **58**, p. 8428 (1998).
- ³ A. Harata, N. Adachi and T. Sawada, *Phys. Rev. B* **58**, p. 7319 (1998).
- ⁴ A. Harata, T. Kawasaki, M. Ito and T. Sawada, *Anal. Chim. Acta* **299**, p. 349 (1995).
- ⁵ A. Harata, T. Edo and T. Sawada, *Chem. Phys. Lett.* **249**, p. 112 (1996).
- ⁶ A. Hibara, A. Harata and T. Sawada, *Chem. Phys. Lett.* **272**, p. 1 (1997).
- ⁷ K. Katayama, T. Sawada, I. Tsuyumoto and A. Harata, *Bull. Chem. Soc. Jpn.* **72**, p. 2383 (1999).
- ⁸ Q. Shen, A. Harata and T. Sawada, *J. Appl. Phys.* **77**, p. 1488 (1995).
- ⁹ S. Ikeda, K. Katayama, I. Tsuyumoto, T. Tanaka, A. Harata and T. Sawada, *J. Chem. Phys.* **111**, p. 9393 (1999).
- ¹⁰ K. Katayama, Y. Inagaki and T. Sawada, *Phys. Rev. B* **61**, p. 7332 (2000).
- ¹¹ A. Othonos, *J. App. Phys.* **83**, p. 1789 (1998).
- ¹² K. Katayama, Y. Inagaki and T. Sawada, *Phys. Rev. B* **61**, p. 7332 (2000).
- ¹³ D. E. Aspnes and A. A. Studna, *Phys. Rev. B* **27**, p. 985 (1983).
- ¹⁴ T. Miyazaki and S. Adachi, *J. Appl. Phys.* **77**, p. 1741 (1995).
- ¹⁵ H. Neddermeyer, U. Misse and P. Rupieper, *Surf. Sci.* **117**, p. 405 (1982).
- ¹⁶ F. J. Himpsel and Th. Fauster, *J. Vac. Sci. Technol. A* **2**, p. 815 (1984).
- ¹⁷ M. Fujita, H. Nagayoshi and A. Yoshimori, *Surf. Sci.* **208**, p. 155 (1989).
- ¹⁸ J. Bokor, R. Storz, R. R. Freeman and P. H. Bucksbaum, *Phys. Rev. Lett.* **57**, p. 881 (1986).
- ¹⁹ N. J. Halas and J. Bokor, *Phys. Rev. Lett.* **62**, p. 1679 (1989).
- ²⁰ M. W. Rowe, H. Liu, G. P. Williams, Jr. and R. T. Williams, *Phys. Rev. B* **47**, p. 2048 (1993).